MOLECULAR IMAGING AND BIOLOGY

Mol Imaging Biol (2019) 21:1138–1146
DOI: 10.1007/s11307-019-01327-4

Published Online: 27 February 2019

WMIS World Molecular Imaging Society

Check for updates

RESEARCH ARTICLE

Evaluation of L-1-[^{18}F]Fluoroethyl-Tryptophan for PET Imaging of Cancer

Yangchun Xin,[1,2] Xiaofei Gao,[3] Li Liu,[1] Woo-Ping Ge,[3] Manoj K. Jain,[4] Hancheng Cai[1,4,5]

[1]*Department of Radiology, University of Texas Southwestern Medical Center, Dallas, TX, 75390, USA*
[2]*Katzin Diagnostic & Research PET/MR Center, Nemours/Alfred I. DuPont Hospital for Children, Wilmington, DE, 19803, USA*
[3]*Children's Research Institute, Department of Pediatrics, Neuroscience, Neurology & Neurotherapeutics, Harold C. Simmons Comprehensive Cancer Center, University of Texas Southwestern Medical Center, Dallas, TX, 75390, USA*
[4]*Department of Radiology, Mayo Clinic, Jacksonville, FL, 32224, USA*
[5]*Advanced Imaging Research Center, University of Texas Southwestern Medical Center, Dallas, TX, 75390, USA*

Abstract

Purpose: Fluorine-18 labeled tryptophan analog L-1-[^{18}F]fluoroethyl-tryptophan (L-1-[^{18}F]FETrp) was designed for positron emission tomography (PET) imaging of cancer by dual targeting of the overexpressed amino acid transporters and altered indoleamine 2,3-dioxygenase (IDO)-mediated kynurenine pathway of tryptophan metabolism. In our previous study, we described the radiosynthesis and preliminary evaluation of L-1-[^{18}F]FETrp for PET imaging of breast cancer. The aim of this study was to investigate the *in vivo* imaging mechanism and further evaluate this radiotracer in more wide range types of cancers including prostate cancer, lung cancer, and glioma.

Procedures: The mice bearing subcutaneous PC-3 prostate cancer, subcutaneous H2009 and H460 lung cancers, subcutaneous MDA-MB-231, orthotopic A549 lung cancer, and intracranial 73C glioma were employed to evaluate L-1-[^{18}F]FETrp for PET imaging of cancer. The *in vivo* catabolism of L-1-[^{18}F]FETrp in the tumor was studied by analysis of PC-3 extracts with radio-HPLC.

Results: Small animal PET/CT imaging of L-1-[^{18}F]FETrp visualized all tumors in these different mouse models with high accumulations of radioactivity in PC-3 (7.5 ± 0.6 % ID/g), H2009 (5.3 ± 0.8 % ID/g), H460 (9.0 ± 1.4 % ID/g), A549 (4.5 ± 0.5 % ID/g), and 73C (4.1 ± 0.7 % ID/g) tumors. The radio-HPLC analysis of PC-3 tumor extracts revealed that about 30 % of L-1-[^{18}F]FETrp was converted into a highly polar radioactive metabolite. The uptake in H460 cancer was about 1.7-fold higher than that in H2009 cancer, which indicated L-1-[^{18}F]FETrp could differentiate these subtypes of lung cancers (H2009 and H460) by imaging quantification. Furthermore, small animal PET/CT imaging in intracranial glioma revealed L-1-[^{18}F]FETrp could pass blood-brain barrier (BBB) and accumulate in glioma with a favorable imaging contrast (tumor-to-brain 2.9).

Conclusions: L-1-[^{18}F]FETrp highly accumulated in a wide range of malignancies including lung cancer, prostate cancer, and glioma. These results suggested that L-1-[^{18}F]FETrp is a promising radiotracer for PET imaging of cancer.

Key Words: PET, Tryptophan metabolism, IDO, Kynurenine pathway, Cancer imaging

Electronic supplementary material The online version of this article (https://doi.org/10.1007/s11307-019-01327-4) contains supplementary material, which is available to authorized users.

Correspondence to: Hancheng Cai; *e-mail:* cai.hancheng@mayo.edu

Introduction

Tryptophan is transported into tumor cells primarily through L-type amino acid transporter (LAT) and further catabolized into several bioactive metabolites mainly through intracellular rate-limiting enzymes indoleamine 2,3-dioxygenase/tryptophan 2,3-dioxygenase (IDO/TDO)-mediated kynurenine pathway, which can regulate immune response by suppressing T cell function and allow tumor immune escape [1, 2]. Given the importance of kynurenine pathway of tryptophan metabolism in numerous cancers, the kynurenine pathway is increasingly recognized as a prominent target for cancer imaging and therapy [3–6]. For instance, several IDO inhibitors have being investigated as a single agent or combination with other therapies for treatment of a wide range of primary or metastatic cancers including breast, prostate, lung, melanoma, pancreas, ovarian, and brain tumors in multiple clinical trials [7–10]. In particular, these IDO inhibitors serve as immunometabolic adjuvants that enhance systemic immune responses with combination immunotherapy of programmed cell death protein 1/programmed death-ligand 1/(PD-1/PD-L1) antibody drugs, leading to promising results in clinical trials [11, 12]. However, selecting right patients for this type of combination immunotherapy and monitoring the cancer immunotherapy response are difficult due to the lack of validated biomarkers.

Positron emission tomography (PET) is a noninvasive and quantitative imaging technique and it allows the functional evaluation of cancer-associated metabolic abnormalities [13]. PET imaging of IDO-mediated kynurenine pathway of tryptophan metabolism may provide valuable information for monitoring IDO inhibitor-based combination cancer immunotherapy. Currently, radiotracer alpha-[11C]methyl-L-tryptophan ([11C]AMT) is used for PET imaging of IDO-mediated kynurenine pathway in clinical research [14]. However, this radiotracer is limited to a few PET centers due to its short half-life (20 min) and the complicated radiosynthesis [15]. Recently, a number of fluorine-18 labeled tryptophan analogs have been developed for cancer imaging, including L-1-[18F]fluoroethyl-tryptophan (L-1-[18F]FETrp), however, none of them has been translated to clinic PET imaging of cancer [16–22]. Among these radiotracers, Dr. Henrottin's group and our group have identified and prepared L-1-[18F]FETrp for PET imaging of IDO-mediated kynurenine pathway [16–18]. In these studies, we have described the development of a practical method for the automated radiosynthesis of L-1-[18F]FETrp, and our biological evaluation results suggest that L-1-[18F]FETrp is a promising radiotracer for PET imaging of IDO-mediated kynurenine pathway of tryptophan metabolism in a breast cancer mouse model [16]. Furthermore, our comparative study between L-1-[18F]FETrp and [11C]AMT in patient derived tumor xenograft mouse models showed the advantages of L-1-[18F]FETrp over [11C]AMT in terms of tumoral uptake, tumor-to-background ratio and radiotracer availability [17].

Our previous study has demonstrated L-1-[18F]FETrp influx into breast cancer cells predominantly *via* overexpressed amino acid transporters LAT and alanine-, serine-, and cysteine-preferring (ASC), and the tumor cell uptake is associated with IDO expression [16]. However, there is lack of evidence of L-1-[18F]FETrp *in vivo* catabolism in IDO overexpressed cancers. Moreover, we need to validate the imaging findings in other common cancers with high IDO expression. In the present study, we investigated the metabolic stability of L-1-[18F]FETrp in cancer and its "trapping mechanism", and further evaluated this radiotracer as a cancer imaging agent in more wide range types of cancer mouse models including subcutaneous PC-3 prostate cancer, subcutaneous H2009 and H460 lung cancers, orthotopic A549 lung cancer, and intracranial 73C glioma.

Materials and Methods

Radiosysnthesis of L-1-[18F]FETrp, Cell Lines, and Animal Models

Radiotracer L-1-[18F]FETrp with a molar activity of 495.43 ± 129.5 GBq/μmol ($n = 7$) was obtained using a one-pot two-step procedure in GE FX-N module following our previously reported method [16]. Carcinomas cell lines PC-3, H2009, H460, and A549 were obtained from the American Type Culture Collection (ATCC, Manassas, VA). Mouse astrocytes derived glioma cell line 73C with BRAFV600E, Pten −/−, P53 −/−, was kindly provided by Dr. Robert M Bachoo Laboratory. Male SCID mice (6–8 weeks of age) were purchased from the Wakeland Mouse Breeding Core at the UT Southwestern Medical Center. Nude mice were purchased from the NCI or Jackson laboratory. The preparation of subcutaneous PC-3 tumor model, subcutaneous H2009 and H460 tumor model, subcutaneous MDA-MB-231 tumor model, orthotopic A549 lung tumor model, and intracranial 73C glioma mouse model is detailed in the Electronic Supplementary Material and in compliance with the Guidelines for the Care and Use of Research Animals established by the UT Southwestern Medical Center Animal Use Committee. Detailed procedures for the radiosynthesis of L-1-[18F]FETrp, cell culture, and animal model preparation are presented in the supplemental materials.

Animal Studies

After the intravenous injection of 3.7–7.4 MBq of L-1-[18F]FETrp in ~ 150 μl of saline, mice were subjected to the small animal positron emission tomography/computed tomography (micro-PET/CT) scan (Siemens Medical Solutions Inc., Knoxville, TN) under 1–2 % isoflurane anesthesia. Static PET scans were performed for 15 min, immediately followed by a CT scan (10 min). For the PET quantification, tumor and other organs were determined by

CT morphology, and regions of interest (ROIs) were defined manually over their entire volumes. The resulting quantitative data were expressed in percentage injected dose per gram (% ID/g). After the *in vivo* imaging studies, the biodistribution and metabolic stability studies were performed to validate the imaging data. The procedures for biodistribution and metabolic stability studies could be found in supplemental materials.

Statistical Analyses

Statistical analyses were performed using two-way analysis of variance (ANOVA) with GraphPad Prism 7.0 (GraphPad Software, Inc., San Diego, CA). Differences between groups were considered to be significant at a P value of < 0.05.

Results

L-1-[18F]FETrp "Trapping" into a Tumor and Imaging Prostate Cancer with PET

To investigate the "trapping mechanism" of L-1-[18F]FETrp in cancer, we evaluated L-1-[18F]FETrp in PC-3, which produces constitutively IDO activity in culture naturally (25), on cell uptake study and PET imaging, and further compared the results with MDA-MB-231 tumor, where IDO expression was undetectable [16]. L-1-[18F]FETrp uptake in PC-3 cells was continually increasing and up to 7.8 ± 0.1 %/mg within 60 min (Fig. 1a). As expected, L-1-[18F]FETrp uptake increased ~18 % in comparison to our previous results in MDA-MB-231 cells (6.6 ± 0.7 %/mg). Similar to cell uptake results, radioactive uptake of PC-3 tumor on L-1-[18F]FETrp PET imaging at 2 h post-injection (7.5 ± 0.6 % ID/g, Fig. 1b and Suppl. Table 1, see Electronic Supplementary Material (ESM)) was 64 % higher than the corresponding uptake of MDA-MB-231 (4.6 ± 0.4 % ID/g) [16], which was consistent with the *in vitro* cell uptake results.

Based on above results, we further hypothesized that the presence of IDO expression would enhance L-1-[18F]FETrp trapping process in cancer, and thus increase the imaging contrast (tumor-to-muscle ratio) at later time point. Therefore, we scanned PC-3 tumor bearing mice at 4 h post-injection. It was found that L-1-[18F]FETrp uptake of PC-3 tumor on PET/CT image was still in a relatively high level (6.4 ± 1.0 % ID/g) at 4 h. These imaging results were further validated by *ex vivo* biodistribution data (5.7 ± 0.6 % ID/g, Suppl. Table 2, see ESM). The PC-3 tumor uptake at 4 h slightly decreased in comparison with that at 2 h, while, the imaging contrast (tumor-to-muscle ratio) was increased from 4.3 at 2 h to 4.9 at 4 h (Suppl. Table 1). The increased imaging contrast is probably due to a lower background at later time point, IDO-promoted trapping enhancement and radioactive metabolites transport.

According to IDO-mediated kynurenine pathway of tryptophan metabolism, L-1-[18F]FETrp trapping in tumor cells either binds to the enzyme IDO or undergoes catabolism to its radioactive metabolites within tumor cells. Therefore, it is of great interest to assess whether there is radioactive metabolite formed in tumor tissue. Since the cold standard of the potential metabolite L-1-[18F]FEt-*N*-formyl-kynurenine was not available in our lab, we conducted the metabolism study under a similar radio-HPLC condition as previously used for L-1-FETrp metabolism study [23] in order to estimate the indenity of radio-metabolites. The radio-HPLC study of PC-3 tumor extracts (Supplemental Fig. 1) revealed that about 30 % of L-1-[18F]FETrp was converted to a more hydrophilic radioactive metabolite (retention time 4.6 min) compared parent radiotracer (retention time 11.2 min). Taking into account the fact that the retention time of L-1-FETrp and its metabolite L-1-FEt-*N*-formyl-kynurenine was 9.2 min and 5.0 min, respectively, under similar HPLC condition [23], we might conclude that this radioactive metabolite was L-1-[18F]FEt-*N*-formyl-kynurenine or L-1-[18F]FEt-kynurenine. The observed radioactive metabolite suggested that the biotransformation of L-1-[18F]FETrp was involved in the tumor uptake.

PET Imaging of Lung Cancer with L-1-[18F]FETrp

Like prostate cancer, overexpressed LAT and ASC and dysregulated IDO-mediated kynurenine pathway were found in many lung tumors [4, 5]. Non-small cell lung cancers H2009 and H460 are commonly used for PET radiotracer evaluation and H460 has a high IDO expression [24]. Therefore, we also evaluated L-1-[18F]FETrp for PET imaging of cancer in animal models bearing both lung tumors H2009 and H460. As shown in Fig. 2 a, the cell uptakes of L-1-[18F]FETrp were higher in H460 (30 min, 10.6 ± 1.9 %/mg; 60 min, 15.6 ± 3.4 %/mg) than these in H2009 (30 min, 8.3 ± 1.0 %/mg; 60 min, 10.2 ± 1.0 %/mg). Micro-PET/CT imaging with L-1-[18F]FETrp acquired at 2 h post-injection showed that the accumulations of L-1-[18F]FETrp in H2009 lung tumor (5.3 ± 0.8 % ID/g) and H460 lung tumor (9.0 ± 1.4 % ID/g) were much higher than that in normal lung tissue (1.6 ± 0.1 % ID/g, $p = 0.0004$ and 0.0002, respectively) (Fig. 2b). Furthermore, L-1-[18F]FETrp uptakes between H2009 tumor and H460 tumor were significantly different, and the radioactive uptake in H460 was about 1.7-fold higher than that in H2009 ($p = 0.0053$), which is in agreement with the cell uptake results (Fig. 2a). Since the H460 tumor has a high IDO expression [24], it is of interest for us to examine the retention of radiotracer with PET in the lung tumors at different time points. The PET imaging on lung tumor xenografts were acquired at 1, 2, 3, and 4 h post-injection. These series imaging revealed a favorite retention of L-1-[18F]FETrp in tumor H460 during 1–4 h (Fig. 2c).

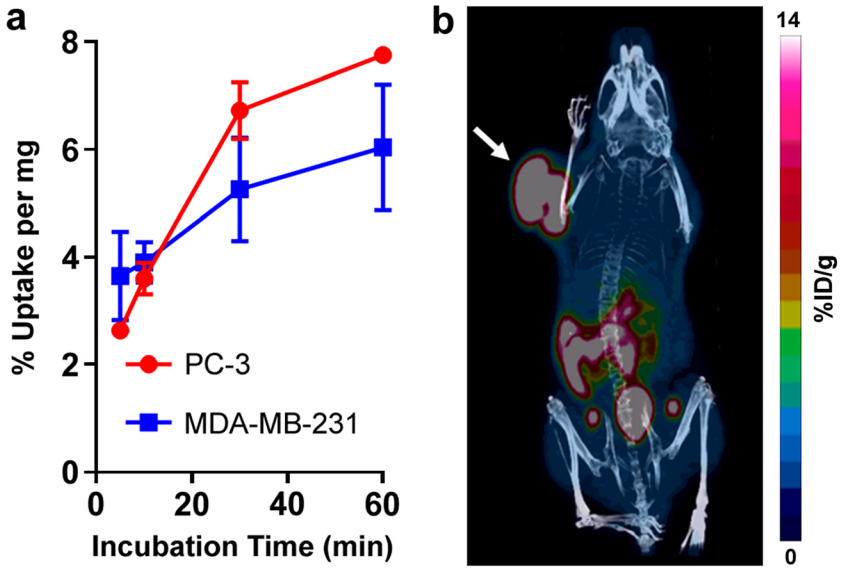

Fig. 1. **a** *In vitro* cell uptake of L-1-[18F]FETrp into PC-3 and MDA-MB-231 cells within 60-min incubation. Data were expressed as percentage of injected dose (% ID) per mg protein ($n = 3–6$). **b** Representative PET/CT image of mice bearing PC-3 tumor xenograft. The mice ($n = 3$) were injected with the L-1-[18F]FETrp into a tail vein and PET data were acquired 2 h post-injection. The PC-3 tumor is marked with a white arrow.

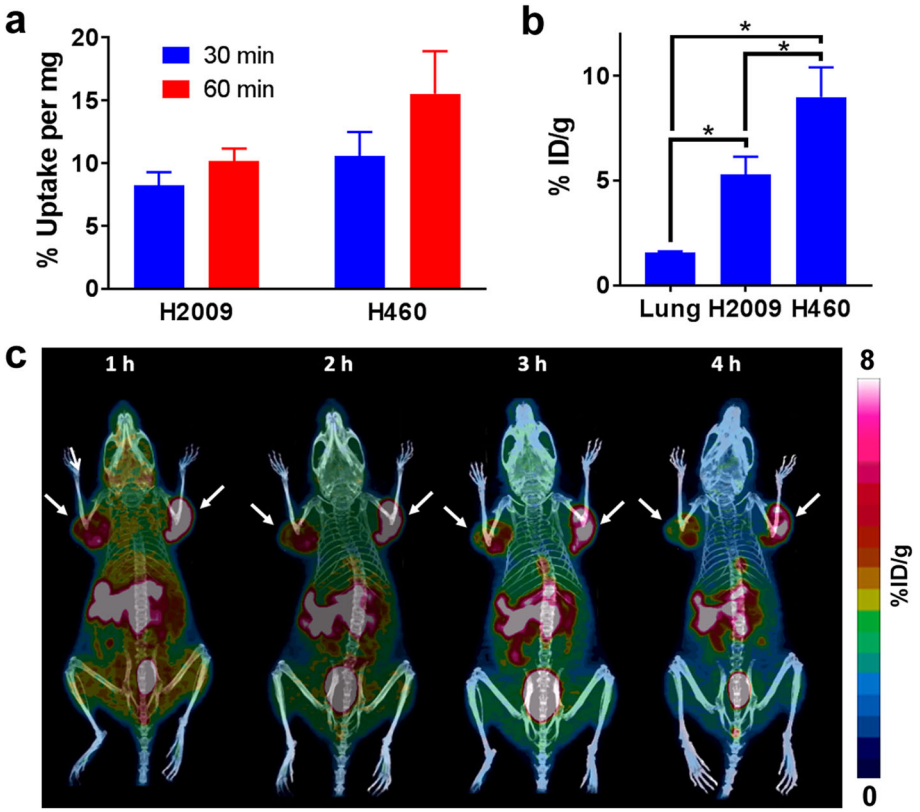

Fig. 2. **a** Radioactive uptake of L-1-[18F]FETrp into H2009 and H460 cells at 30- and 60-min incubation ($n = 6$). **b** Radiotracer accumulations in H2009 tumor, H460 tumor, and normal lung at 2 h post-injection ($n = 3$). The uptakes of radiotracer in both tumors H2009 and H460 were significantly higher than that in normal lung ($P = 0.0004$ and 0.0002, respectively). The uptake of radiotracer in tumor H460 was significantly higher than that in tumor H2009 ($P = 0.0053$). **c** PET images of xenograft-bearing mice with H2009 and H460 lung tumors (left shoulder: H2009 tumor; right shoulder: H460). Xenograft-bearing mice were injected with L-1-[18F]FETrp *via* a tail vein and PET/CT data were acquired at 1, 2, 3, and 4 h post-injection. Tumors are marked with white arrows.

Encouraged by the PET imaging results in lung tumor xenografts, we next evaluated L-1-[18F]FETrp in a mouse model bearing orthotropic lung tumor A549, which was reported to have a high IDO expression [24]. As expected, a high accumulation of the radioactivity (4.5 ± 0.5 % ID/g) was obtained at 2 h post-injection (Fig. 3), and the orthotropic A549 lung tumor was clearly visualized by micro-PET/CT with a favorable imaging contrast (tumoral lung/normal lung) of 2.6. These imaging data demonstrated the high potential of L-1-[18F]FETrp PET for imaging lung cancer in clinic.

PET Imaging of Brain Cancer with L-1-[18F]FETrp

In our study, we observed the normal brain uptake of L-1-[18F]FETrp was low during 5- to 60-min dynamic imaging, which provided a favorable low brain imaging background, but also might be indicative of its low blood-brain barrier (BBB) penetration or quick washout from the brain. Low availability of a radiotracer in the brain is commonly indicative of a failure in the development of neuroimaging agents. It is still unknown if the low uptake of L-1-[18F]FETrp in normal brain during 5–60 min will limit the brain tumor imaging.

In order to assess whether L-1-[18F]FETrp could pass BBB and accumulate in brain tumor, we evaluated PET imaging of brain tumor with L-1-[18F]FETrp in an intracranial glioma mouse model. Our micro-PET imaging results (Fig. 4a, b) revealed L-1-[18F]FETrp could pass BBB, and accumulated in 73C glioma (4.1 ± 0.7 % ID/g) with a favorable imaging contrast (tumor-to-brain 2.9). After PET imaging, mouse brains were sliced and the location of 73C glioma was further confirmed through GFP fluorescence by fluorescent microscopy imaging (Fig. 4c). These results demonstrated that L-1-[18F]FETrp had a good BBB permeability and high potential for the imaging of brain tumor.

Discussion

L-1-[18F]FETrp "Trapping" into a Tumor

Tryptophan is used in the biosynthesis of proteins and bioactive metabolites in cell metabolism and involved in three major metabolism pathways in humans, including protein synthesis, serotonin pathway, and kynurenine pathway. Among them, kynurenine pathway accounts for ~ 95 % of tryptophan metabolism. Radiotracer L-1-[18F]FETrp was designed for PET imaging of cancer by dual targeting of the amino acid transporters (LAT and ASC) and IDO-mediated kynurenine pathway of tryptophan metabolism. Given that L-1-[18F]FETrp is structurally similar to tryptophan and an IDO inhibitor/substrate 1-methyl-L-trytophan, we hypothesize that L-1-[18F]FETrp can cross tumor cell membrane through overexpressed amino acid transporters LAT and ASC, and then binds to IDO enzyme, and subsequently undergoes its catabolism in the cells (Fig. 5). Because of the nature of their exchange transport mechanism, LAT and ASC cannot highly concentrate amino acid-based radiotracers in cancer cells, which often leads to a moderate imaging contrast (tumor-to-background ratio) for LAT- or/and ASC-targeted amino acid radiotracers. IDO, a cytosolic enzyme [25], can bind with L-1-[18F]FETrp and catalyze its degradation. This intracellular binding to IDO and subsequent catabolism would contribute to the increased trapping of L-1-[18F]FETrp in cancers and thereby lead to an improved imaging contrast compared to conventional amino acid-based radiotracers. In this study, we validated our hypothesis and further evaluated L-1-[18F]FETrp for PET imaging of cancer, including prostate cancer, lung cancer, and brain cancer.

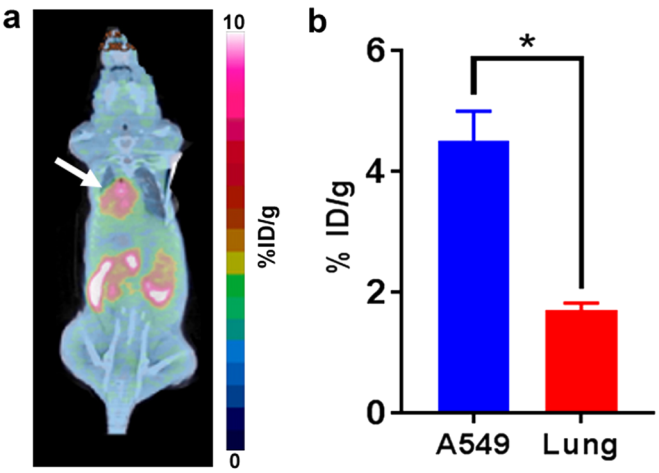

Fig. 3. PET/CT image of orthotopic A549 lung tumor mice. Mice were injected with the L-1-[18F]FETrp through tail vein. PET/CT data were acquired at 2 h post-injection. The lung uptake data were expressed as means ± SD ($n = 3$). The uptake of radiotracer in lung tumor A549 was significantly higher than that in normal lung ($P = 0.0008$).

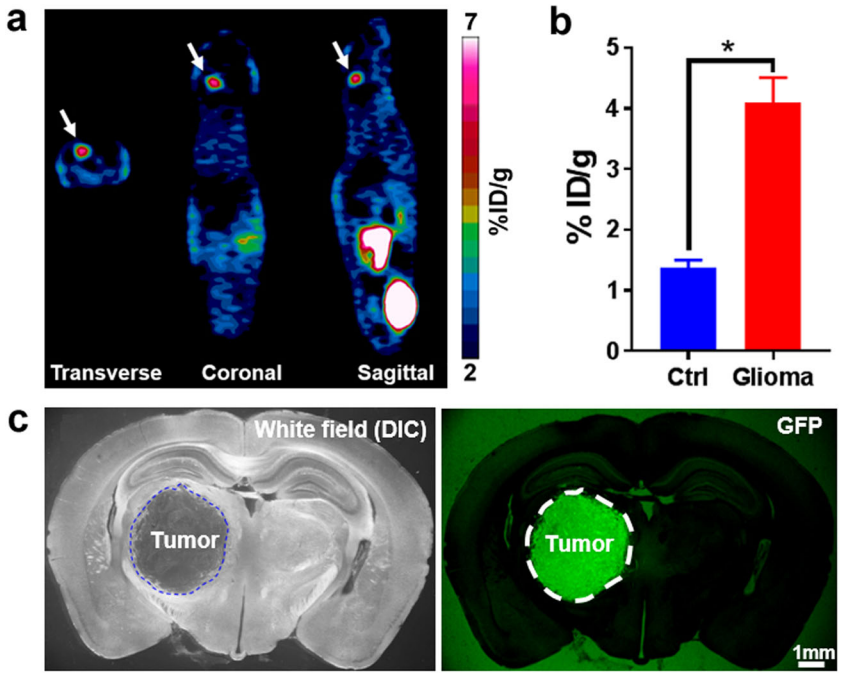

Fig. 4. **a** Representative PET images of intracranial glioma transplanted on mice ($n = 3$). Intracranial brain 73C-glioma transplanted mice were injected with the L-1-[18F]FETrp into a tail vein. PET data were acquired 2 h post-injection. The glioma is marked with white arrows. **b** The radioactive uptake qualification of 73C glioma and normal brain 2 h post-injection. The uptake of radiotracer in glioma was significantly higher than that in normal brain ($P = 0.0030$). **c** 73C-GFP glioma in mouse brain, both DIC and fluorescent images show the tumor in thalamus-stratum region.

The *in vitro* enzymatic assay has proved standard compound L-1-FETrp is an IDO substrate [23]. Our previous study also demonstrated that L-1-[18F]FETrp was transported into cancer cells predominantly through overexpressed amino acid transporters LAT and ASC, and the accumulation in cancer cells was associated with intracellular IDO expression, which was exemplified in breast cancer MDA-MB-231 cells with and without interferon-gamma treatment [16]. In this study, we further found that L-1-[18F]FETrp has a higher uptake in high-IDO expressing tumor cells (PC-3) as compared to low-IDO expressing tumor cells (MDA-MB-231). This findings were consistent with results from a recent report that demonstrated L-1-[18F]FETrp uptakes in tumor cells were correlated with different levels of IDO expression [18]. To our best knowledge, there was, so far, no *in vivo* study of L-1-[18F]FETrp on tumors with different levels of IDO expression. Our PET imaging results showed that L-1-[18F]FETrp uptake in high-IDO expressing tumor (PC-3) was significantly higher than that in low-IDO expressing tumor (MDA-MB-231), suggesting L-1-[18F]FETrp uptake is likely associated with IDO expression in the tumor. Furthermore, the high uptake of L-1-[18F]FETrp in high-IDO expressing tumors (PC-3 and H460) indicated that a trapping mechanism was involved in the radioactive uptake and retention. In addition, 98 % of L-1-[18F]FETrp remained intact in MDA-MB-231 tumor tissue [16], while, 30 % of L-1-[18F]FETrp was metabolized in PC-3 tumor tissue, giving a radioactive metabolite, which very likely corresponded kynurenine analogs. Collectively, these findings strongly support our proposed IDO-mediated trapping mechanism, which is L-1-[18F]FETrp influx into tumor through overexpressed amino acid transporters LAT and ASC, and further retention or trap within the tumor *via* IDO-mediated kynurenine pathway of tryptophan metabolism (Fig. 5).

PET Imaging of Cancer with L-1-[18F]FETrp

PET imaging performed in mouse tumor models illustrates the potential utility of L-1-[18F]FETrp for imaging of various cancers. Specifically, the low uptake in normal lung and substantial different radioactive uptakes in H2009 and H460 tumors indicate that L-1-[18F]FETrp not only enables to detect lung tumors, but also can differentiate the subtypes of lung tumors H2009 and H460. The high uptake of L-1-[18F]FETrp in H460 tumor is probably due to the high expression of IDO in this tumor. To our best knowledge, the IDO expression level in H2009 was not reported. Therefore, more work is needed to compare the IDO activities on both tumors. Moreover, L-1-[18F]FETrp for PET imaging of lung cancers was further evaluated in more clinic-relevant orthotopic A549 tumor mice. These results clearly demonstrated the potential of L-1-[18F]FETrp PET for cancer imaging in clinic.

Our previous study in subcutaneous patient-derived brain tumor xenografts suggested that L-1-[18F]FETrp is a promising agent for PET imaging of brain tumor [17]. However,

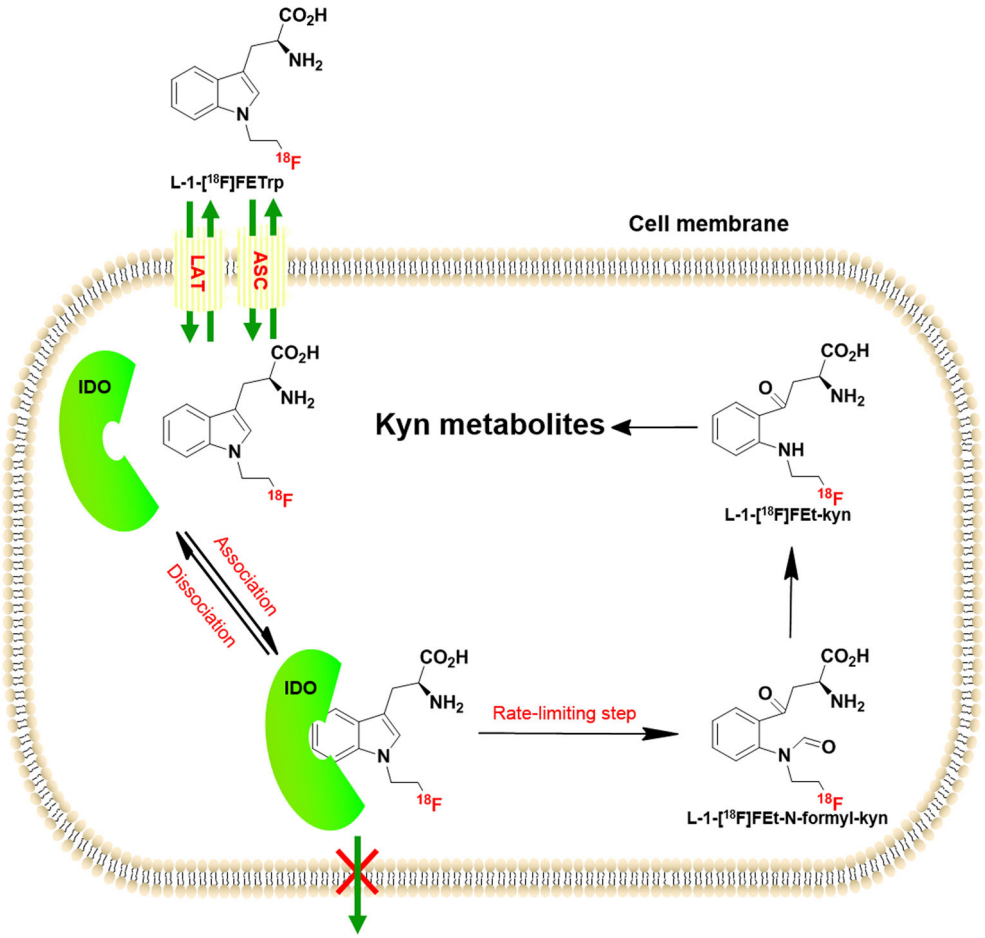

Fig. 5. The proposed mechanism of L-1-[18F]FETrp "trapping" in tumor cell. L-1-[18F]FETrp crosses tumor cell membrane through exchange amino acid transporters LAT and ASC, then binds to IDO enzyme, forming an IDO-radiotracer complex, which cannot pass through cell membrane. The IDO-radiotracer complex either releases free L-1-[18F]FETrp or yields L-1-[18F]FEt-*N*-formyl-kyn, which might be further catabolized into Kyn metabolites in the cells. L-1-[18F]FETrp is trapped in the tumor cell mainly due to the binding to IDO enzyme and further catabolism.

its BBB permeability is still our special concern. Thus, we evaluated PET imaging of L-1-[18F]FETrp in an intracranial glioma mouse model, and found that L-1-[18F]FETrp could pinpoint the tumor in the brain. This study clearly demonstrated the potentials of L-1-[18F]FETrp for PET imaging of brain tumor in clinic and also indicated its applications in other brain diseases with altered kynurenine pathway of tryptophan metabolism.

Given its low uptake in normal lung and brain, as well as favorable kinetics and radiation dosimetry [17], the imaging results of L-1-[18F]FETrp in this study strongly support the clinical translation for both lung cancer and brain tumor. Although the application of L-1-[18F]FETrp PET in primary prostate tumor may be still limited because of its high accumulation in the surrounding of prostate, such as urinary bladder that increases gradually over time, but it may find application in assessment of prostate cancer recurrence at early imaging time point as recent FDA-approval PET drug amino acid analog Axumin (F-18 fluciclovine) injection does [26]. In addition to diagnosis of various cancers, L-1-[18F]FETrp PET may serve as a novel research tool for monitoring IDO-targeted therapy response. For instance, the results from a phase 2 clinic trial have showed a significant improvement in radiographic and clinical progression by treatment with IDO inhibitor indoximod post-sipuleucel-T therapy in patients with metastatic castration resistant prostate cancer. However, current biomarkers failed to monitor the augmentation of immune response with IDO inhibition [27, 28]. L-1-[18F]FETrp PET may have potential to serve as an imaging biomarker for monitoring IDO inhibitor-based immunotherapy in clinic. Moreover, amino acid transporters LAT and ASC are highly expressed in wide range of human cancers including breast cancer, prostate cancer, lung cancer, and brain tumor, responsible for cancer initiation, progression, and metastasis [29, 30]. Therefore, L-1-[18F]FETrp PET also have potentials to facilitate LAT/ASC drug development for cancer diagnosis and therapy.

In summary, L-1-[18F]FETrp PET clearly visualized the breast cancer [16], prostate cancer, lung cancer, and brain cancer [17] in various animal models, demonstrated the

potential for further clinical translation. Moreover, the observed *in vivo* metabolism of L-1-[^{18}F]FETrp in PC-3 tumor and favorable retention of radioactivity in these tumors suggested that biotransformation of radiotracer is implicated in the radioactive uptake, which support that IDO-mediated kynurenine pathway of tryptophan metabolism was involved in enhancement of radioactivity accumulation. A limitation of this study is the lack of direct quantitative comparison of IDO and TDO expressions in these tumors and thus to what extent the altered kynurenine pathway affects the L-1-[^{18}F]FETrp uptake and retention is still unclear. Further studies on correlation of L-1-[^{18}F]FETrp uptake with IDO and TDO activity as well as the expression of amino acid transporters (LAT and ASCT) on these tumors are needed.

Conclusion

L-1-[^{18}F]FETrp highly accumulates in a wide range of malignancies including lung cancer, prostate cancer, and gliomas. The biotransformation of L-1-[^{18}F]FETrp occurs in the tumor with high IDO expression. L-1-[^{18}F]FETrp is a promising radiotracer for PET imaging of cancers by dual targeting of the amino acid transporters (LAT and ASC) and IDO-mediated kynurenine pathway of tryptophan metabolism.

Acknowledgments. We are grateful to Prof. Xiankai Sun and Dr. Aditi Mulgaonkar in UTSW for providing scientific insights and experimental supports. We also would like to thank Robert Hallgren in UTSW for producing [^{18}F]F$^-$ ion used in radiotracer synthesis.

Funding Information. This work was financially supported by the UT Southwestern Simmons Cancer Center Grant (NIH 5P30 CA 142543), the American Cancer Society and the Simmons Cancer Center (ACS-IRG-02-196), the UT Southwestern High Impact/High Risk funds, NINDS K99/R00 (R00NS073735), the Jonesville Foundation and CRI start-up funds to W.P.G.

Compliance with Ethical Standards

Conflict of Interest

The authors declare that they have no conflict of interest.

References

1. Vécsei L, Szalárdy L, Fülöp F, Toldi J (2013) Kynurenines in the CNS: recent advances and new questions. Nat Rev Drug Discov 12:64–82
2. Dounay AB, Tuttle JB, Verhoest PR (2015) Challenges and opportunities in the discovery of new therapeutics targeting the kynurenine pathway. J Med Chem 58:8762–8782
3. Plathow C, Weber WA (2008) Tumor cell metabolism imaging. J Nucl Med 49:43S–63S
4. Karanikas V, Zamanakou M, Kerenidi T, Dahabreh J, Hevas A, Nakou M, Gourgoulianis KI, Germenis AE (2007) Indoleamine 2,3-dioxygenase (IDO) expression in lung cancer. Cancer Biol Ther 6:1258–1262
5. Uyttenhove C, Pilotte L, Théate I, Stroobant V, Colau D, Parmentier N, Boon T, van den Eynde BJ (2003) Evidence for a tumoral immune resistance mechanism based on tryptophan degradation by indoleamine 2,3-dioxygenase. Nat Med 9:1269–1274
6. Astigiano S, Morandi B, Costa R, Mastracci L, D'Agostino A, Ratto GB, Melioli G, Frumento G (2005) Eosinophil granulocytes account for indoleamine 2,3-dioxygenase-mediated immune escape in human non-small cell lung cancer. Neoplasia 7:390–396
7. Moon YW, Hajjar J, Hwu P, Naing A (2015) Targeting the indoleamine 2,3-dioxygenase pathway in cancer. J Immunother Cancer 3:51
8. Brochez L, Chevolet I, Kruse V (2017) The rationale of indoleamine 2,3-dioxygenase inhibition for cancer therapy. Eur J Cancer 76:167–182
9. Perez RP, Riese MJ, Lewis KD, Saleh MN, Adil Daud JB (2017) Epacadostat plus nivolumab in patients with advanced solid tumors: preliminary phase I/II results of ECHO-204 [ASCO abstract 3003]. J Clin Oncol 35:3003–3003
10. Zakharia Y, McWilliams R, Shaheen M, Grossman K, Drabick J, Milhem M, Rixie O, Khleif S, Lott R, Kennedy E, David Munn NV, CL (2017) Interim analysis of the phase 2 clinical trial of the IDO pathway inhibitor indoximod in combination with pembrolizumab for patients with advanced melanoma. [AACR abstract CT117]. Cancer Res 77(13 Suppl):AM2017–ACT117
11. Platten M, von Knebel Doeberitz N, Oezen I et al (2015) Cancer immunotherapy by targeting IDO1/TDO and their downstream effectors. Front Immunol 5:1–7
12. Godin-Ethier J, Hanafi LA, Piccirillo CA, Lapointe R (2011) Indoleamine 2,3-dioxygenase expression in human cancers: clinical and immunologic perspectives. Clin Cancer Res 17:6985–6991
13. Hanahan D, Weinberg RA (2011) Hallmarks of cancer: the next generation. Cell 144:646–674
14. Juhász C, Muzik O, Lu X et al (2009) Quantification of tryptophan transport and metabolism in lung tumors using PET. J Nucl Med 50:356–363
15. Huang X, Xiao X, Gillies RJ, Tian H (2016) Design and automated production of 11C-alpha-methyl-l-tryptophan (11C-AMT). Nucl Med Biol 43:303–308
16. Xin Y, Cai H (2017) Improved radiosynthesis and biological evaluations of L- and D-1-[18F]fluoroethyl-tryptophan for PET imaging of IDO-mediated kynurenine pathway of tryptophan metabolism. Mol Imaging Biol 19:589–598
17. Michelhaugh SK, Muzik O, Guastella AR, Klinger NV, Polin LA, Cai H, Xin Y, Mangner TJ, Zhang S, Juhász C, Mittal S (2017) Assessment of tryptophan uptake and kinetics using 1-(2- 18 F-fluoroethyl)-l-tryptophan and α- 11 C-methyl-l-tryptophan PET imaging in mice implanted with patient-derived brain tumor xenografts. J Nucl Med 58:208–213
18. Henrottin J, Lemaire C, Egrise D, Zervosen A, Van den Eynde B, Plenevaux A, Franci X, Goldman S, Andr'Luxen E, Luxen A, Jean Henrottin CL et al (2016) Fully automated radiosynthesis of 1-[18F]FETrp, a potential substrate for indoleamine 2,3-dioxygenase PET imaging. Nucl Med Biol 43:379–389
19. Sun T, Tang G, Tian H, Wang X, Chen X, Chen Z, Wang SC (2012) Radiosynthesis of 1-[18F]fluoroethyl-L-tryptophan as a novel potential amino acid PET tracer. Appl Radiat Isot 70:676–680
20. Kramer SD, Mu L, Muller A, Keller C, Kuznetsova OF, Schweinsberg C, Franck D, Muller C, Ross TL, Schibli R, Ametamey SM (2012) 5-(2-18F-fluoroethoxy)-L-tryptophan as a substrate of system L transport for tumor imaging by PET. J Nucl Med 53:434–442
21. Chiotellis A, Mu A, Ro SL et al (2016) Synthesis, radiolabeling, and biological evaluation of 5-hydroxy- 2-[18F]fluoroalkyl-tryptophan analogues as potential PET radiotracers for tumor imaging. J Med Chem 59:5324–5340
22. Zlatopolskiy BD, Zischler J, Urusova EA et al (2018) Discovery of 7-[18 F]fluorotryptophan as a novel positron emission tomography (PET) probe for the visualization of tryptophan metabolism in vivo. J Med Chem 61:189–206
23. Henrottin J, Zervosen A, Lemaire C, Sapunaric F, Laurent S, van den Eynde B, Goldman S, Plenevaux A, Luxen A (2015) N1-fluoroalkyltryptophan analogues: synthesis and in vitro study as potential substrates for indoleamine 2,3-dioxygenase. ACS Med Chem Lett 6:260–265

24. Park GM, Lee S-M, Yim J-J, Yang S-C, Yoo CG, Lee C-T, Han SK, Young-Soo Shim YWK (2009) Expression of COX-2 and IDO by uteroglobin transduction in NSCLC cell lines transduction in NSCLC cell lines. Tuberc Respir Dis (Seoul) 66:274–279
25. Kudo Y, Boyd CAR (2000) Human placental indoleamine 2,3-dioxygenase: cellular localization and characterization of an enzyme preventing fetal rejection. Biochim Biophys Acta - Mol Basis Dis 1500:119–124
26. Bach-Gansmo T, Nanni C, Nieh PT, Zanoni L, Bogsrud TV, Sletten H, Korsan KA, Kieboom J, Tade FI, Odewole O, Chau A, Ward P, Goodman MM, Fanti S, Schuster DM, Willoch F (2017) Multisite experience of the safety, detection rate and diagnostic performance of fluciclovine (18F) positron emission tomography/computerized tomography imaging in the staging of biochemically recurrent prostate Cancer. J Urol 197:676–683
27. Jha GG, Gupta S, Tagawa ST, Koopmeiners JS, Vivek S, Dudek AZ, Cooley SA, Blazar BR, JSM (2017) A phase II randomized, double-blind study of sipuleucel-T followed by IDO pathway inhibitor, indoximod, or placebo in the treatment of patients with metastatic castration resistant prostate cancer (mCRPC). J Clin Oncol 35:3066–3066
28. Masonic Cancer Center, University of Minnesota. Phase II Study of Sipuleucel-T and Indoximod for Patients With Refractory Metastatic Prostate Cancer. Available from: https://clinicaltrials.gov/ct2/show/NCT01560923. NLM identifier: NCT01560923. Accessed 21 Feb 2019
29. Wang Q, Holst J (2015) L-type amino acid transport and cancer: targeting the mTORC1 pathway to inhibit neoplasia. Am J Cancer Res 5:1281–1294
30. Fuchs BC, Bode BP (2005) Amino acid transporters ASCT2 and LAT1 in cancer: partners in crime? Semin Cancer Biol 15:254–266